Supplemental Information

RBP4 activates antigen-presenting cells leading to adipose tissue inflammation and systemic insulin resistance

Pedro M. Moraes-Vieira, Mark M. Yore, Peter M. Dwyer, Ismail Syed, Pratik Aryal, and Barbara B. Kahn

Supplemental Figures

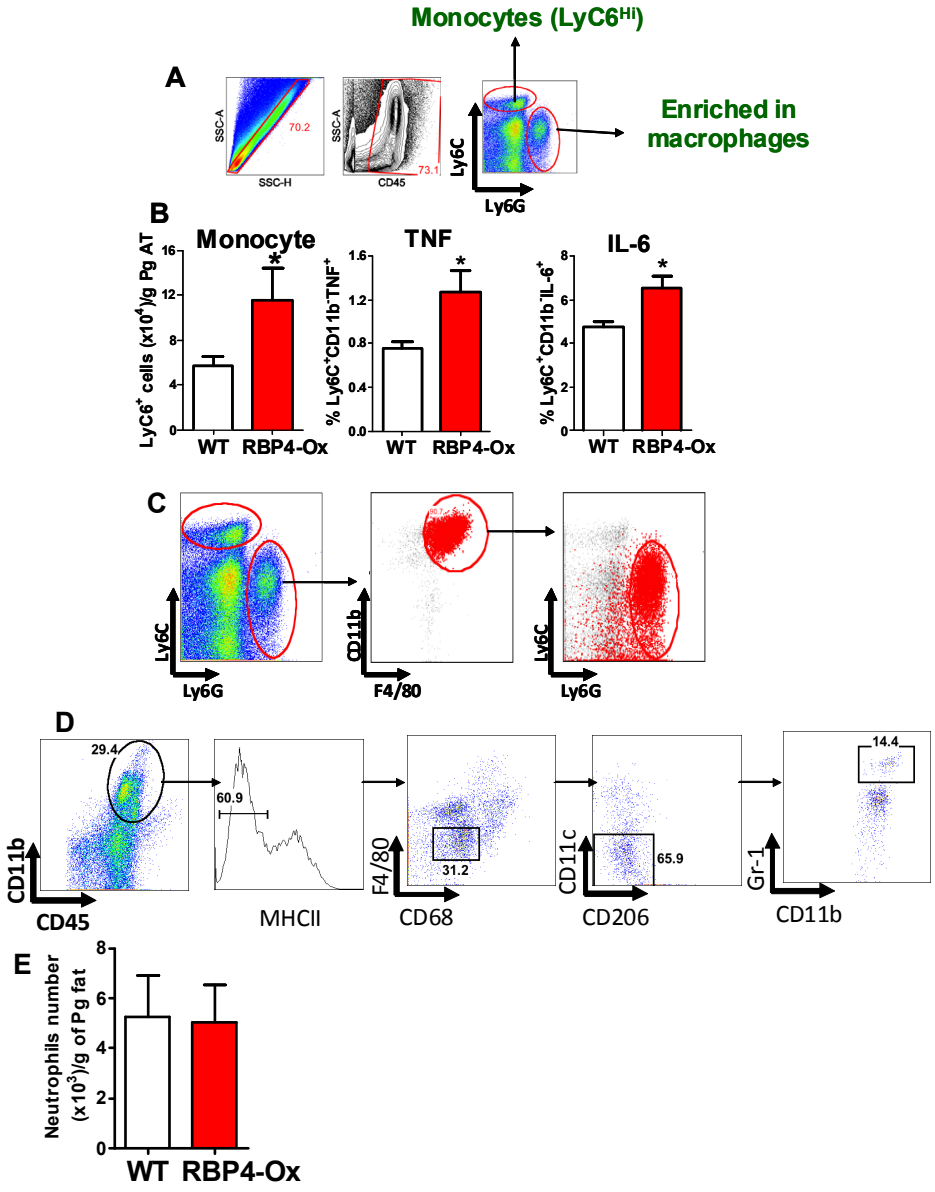

Figure S1, related to Figure 1. Flow cytometry gate strategy and Ly6C$^+$ monocyte and neutrophils levels in perigonadal adipose tissue. (A) Flow cytometry representation of gate strategy for macrophage analysis in WT and RBP4Ox perigonadal (Pg) adipose tissue. Duplets were removed (left panel) and CD45$^+$ AT cells were gated (middle panel). Next, the CD45$^+$ cells were divided into Ly6$^+$Ly6G$^-$ (monocytes) and LyC6-Ly6G$^+$ (enriched in macrophages) populations (right panel). (B) AT monocyte numbers (n=8/group) and TNF and

IL-6 intracellular staining in AT monocytes from WT and RBP4-Ox mice (n=5/group). Data is shown as percentage of total AT monocytes expressing either TNF or IL-6. (C) $Ly6G^+$ adipose tissue leukocytes are enriched in macrophages ($CD11b^+F4/80^+$). Duplets were removed and $CD45^+$ AT cells were gated as shown in (A). Next, the population of $CD45^+$ cells was divided into $Ly6^+Ly6G^-$ (monocytes) and $LyC6^-Ly6G^+$ (enriched in macrophages) populations (right panel). Inside the population of $Ly6C^-Ly6G^+$ cells (left panel) macrophages were defined as $CD11b^+F4/80^+$ (middle panel). Backgate analysis shows the overlay of macrophages back into $Ly6G^+$ cells, demonstrating that this population is enriched in macrophages. (D) AT neutrophil gating strategy. First, we selected cells that are negative for MHCII since neutrophils do not express this marker. To exclude macrophages from this MHCII null population, we further selected for cells negative for the macrophage markers, F4/80 and CD68 and subsequently, cells negative for CD11c and CD206. After these gate exclusions, neutrophils were defined by the expression of Gr-1 and CD11b. (E) AT neutrophil number (n=5/group). Values are means ± standard error. *P<0.05. Pg: perigonadal.

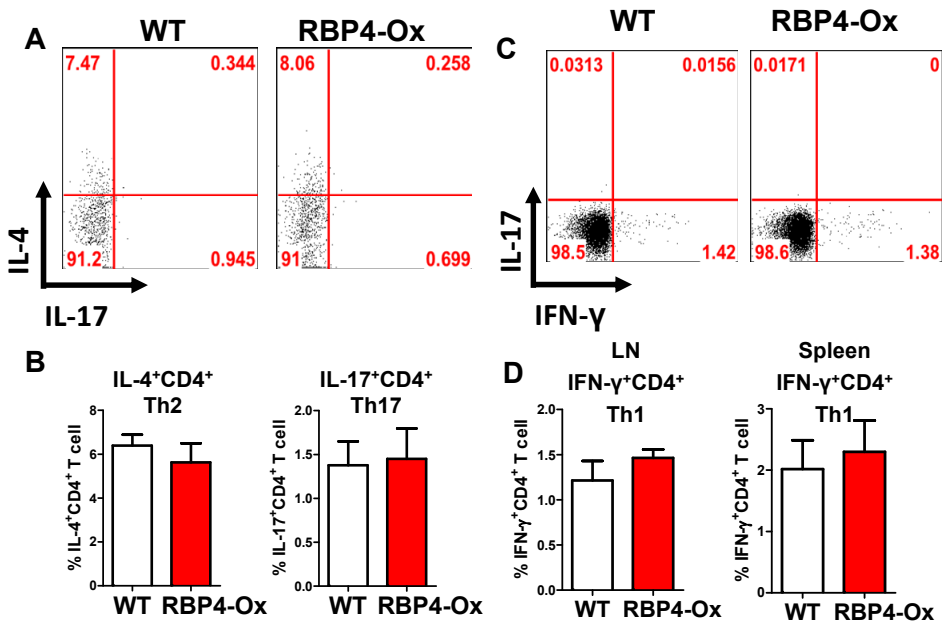

Figure S2, related to Figure 1 and 2. RBP4 overexpression does not increase adipose tissue Th2 and Th17 T cell numbers and does not increase systemic levels of Th1 cells. (A) Flow cytometry representation of gated AT CD4 T cells from WT and RBP4-Ox mice which were intracellularly stained for IL-4 and IL-17. (B) Bar graph representing the percentage of $CD4^{+}IL\text{-}4^{+}$ (Th2) and $CD4^{+}IL\text{-}17^{+}$ (Th17) T cells. (n = 5 per group). (C) Flow cytometry representation of IFN-γ and IL-17 intracellular staining in gated CD4 T cell harvested from mesenteric lymph node. (D) Bar graphs show quantification of the percentage of Th1 in spleen and lymph node of RBP4-Ox and WT mice. (n = 5 per group). Bars are means +/- standard errors.

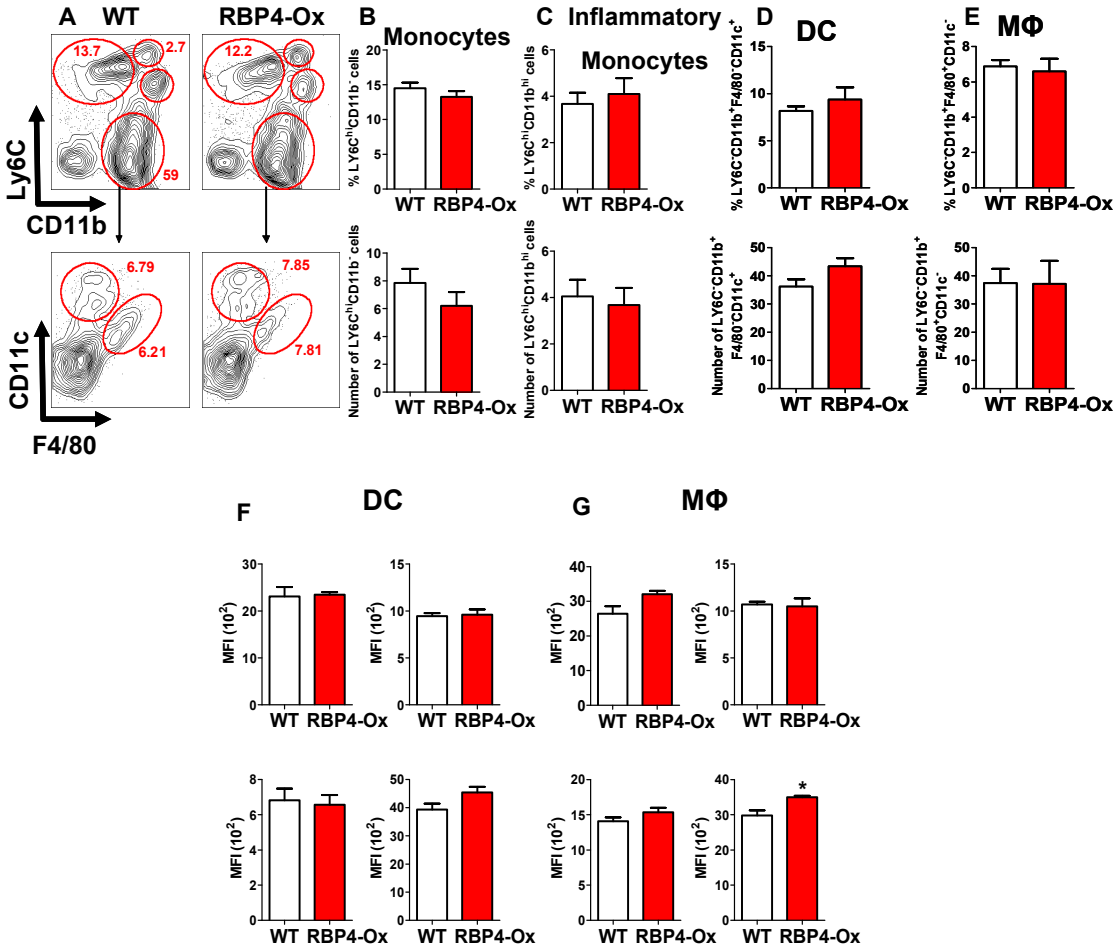

Figure S3, related to Figure 2. RBP4 overexpression does not alter the number or percentage of splenic myeloid cells. (A) Duplets were removed and the cells were divided into monocytes ($Ly6^{+}CD11b^{-}$), inflammatory monocytes ($Ly6^{+}CD11b^{+}$) and $LyC6^{-}CD11b^{+}$ populations. Next, the $CD11b^{+}$ cells were divided into $CD11c^{+}F4/80^{-}$ (dendritic cell) and $CD11c^{-}F4/80^{+}$ (macrophage) cells. (B) Percentage and number of splenic monocytes. (C) Percentage and number of splenic inflammatory monocytes. (D) Percentage and number of splenic dendritic cells. (E) Percentage and number of splenic macrophages (MΦ). (F) Expression of MHCII and co-stimulatory molecules (CD80, CD40, CD86) in dendritic cells. (G) Expression of MHCII and co-stimulatory molecules (CD80, CD40, CD86) in macrophages. n = 5 mice/group. Bars are means +/- standard errors. MFI: Median fluorescence intensity. Similar results were observed for mesenteric lymph node.

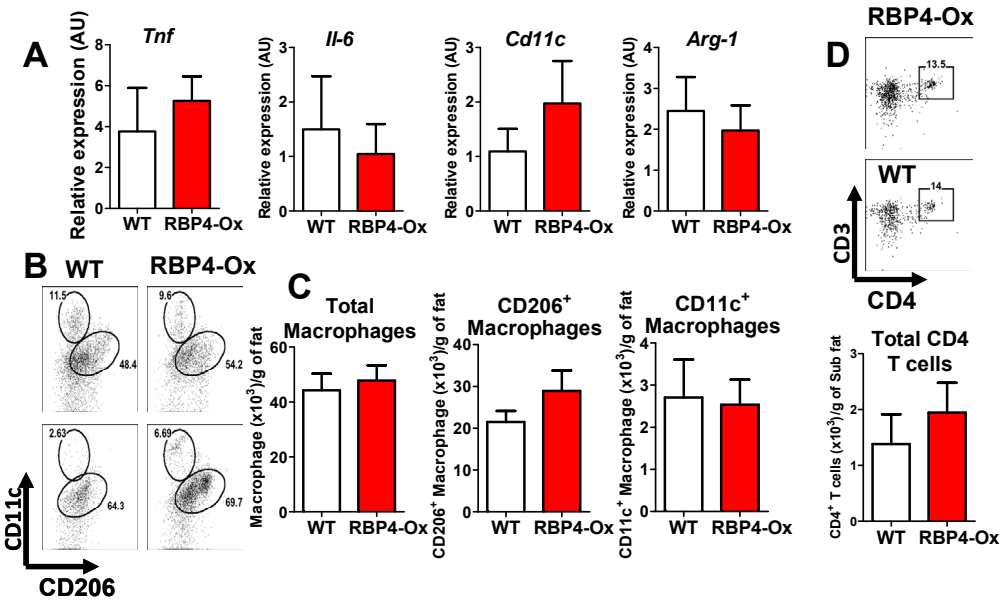

Figure S4, related to Figure 3. Elevated serum RBP4 levels do not result in subcutaneous adipose tissue inflammation in RBP4-Ox mice. (A) RNA was extracted from subcutaneous AT of WT and RBP4-Ox mice. Expression of *Tnf*, *Il-6*, *Cd11c* and *Arg-1* was determined by qPCR (n=6/group). Specific mRNAs are expressed as a ratio to *Gapdh*. (B) Flow cytometry representation (left panel) of $CD11c^+$ and $CD206^+$ subcutaneous adipose tissue macrophages (n=5/group). (C) Number (right panel) of total, $CD11c^+$ or $CD206^+$ subcutaneous adipose tissue macrophages (n=5/group). (D) Flow cytometry representation of subcutaneous adipose tissue $CD4^+$ T cells (upper panel) and total number of subcutaneous adipose tissue $CD4^+$ T cells (bottom panel) (n=5/group). Values are means±standard error.

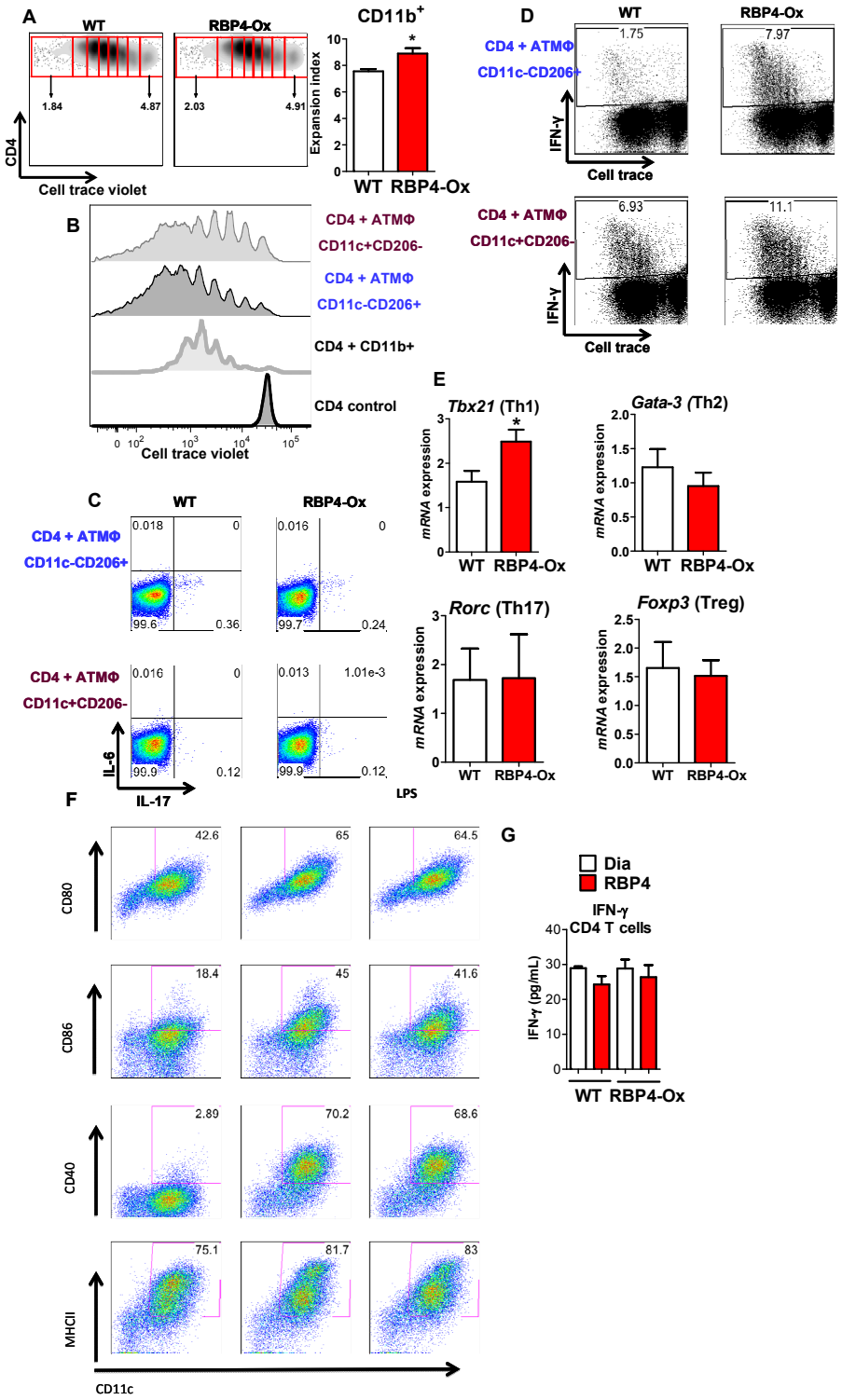

Figure S5, related to Figure 4 and 5. RBP4, antigen proliferation and Th1 polarization. (A) Flow cytometry representation of CD4 T cell proliferation induced by AT CD11b^{+} cells (left and middle panels) and expansion index (right

panel) representing the degree of CD4 T cell proliferation (n=5/group). (B) Flow cytometry histograms of gated CD4 T cells representing cell trace dilution which indicates the extent of CD4 T cell proliferation induced by WT AT $CD11b^+$ cells and by $CD11c^+$ and $CD206^+$ ATMΦ. CD4 control: CD4 T cells not co-cultured with other cell type. (C) $CD11c^+$ and $CD206^+$ ATMΦ were FACS-sorted from adipose tissue from WT and RBP4-Ox and were co-cultured with cell trace-labeled WT splenic CD4 T cells. Th1 polarization was evaluated by IFN-γ intracellular staining in $CD4^+$ T cells and Th1 proliferation by cell trace dilution in $IFN\text{-}\gamma^+CD4^+$ T cells (n=5/group). (D) $CD11c^+$ and $CD206^+$ ATMΦ from WT or RBP4-Ox do not promote Th17 T cell polarization. $CD11c^+$ and $CD206^+$ ATMΦ of WT or RBP4-Ox mice were co-cultured with WT splenic CD4 T cells. Th17 CD4 T cell polarization was evaluated by IL-17 intracellular staining (n=5/group). (E) AT from RBP4-Ox mice express higher levels of the Th1 lineage transcription factor *Tbx21*. RNA was extracted from adipose tissue of WT and RBP4-Ox mice and evaluated by qPCR for the expression of CD4 T lineage transcription factors. *Tbx21*: Th1 transcription factor; *Gata-3*: Th2 transcription factor; *Rorc*: Th17 transcription factor; *Foxp3*: Treg transcription factor (n=5/group). Specific mRNAs are expressed as a ratio to *Gapdh*. (F) Flow cytometry representation of MHCII and co-stimulatory molecules in BMDC. BMDC were generated from WT mice and activated for 24h with RBP4 (50 ug/ml) or LPS (100 ng/ml). Dialysate was used as negative control. The expression of MHCII and co-stimulatory molecules (CD40, CD80 and CD86) was evaluated in $CD11c^+$ cells (BMDC) by flow cytometry (n=5/group). (G) Splenic CD4 T cells from WT or RBP4-Ox mice were stimulated in vitro with RBP4 plus anti-CD3 and the secretion of IFN-γ was evaluated by ELISA (n=5/group). Values are means ± standard error. $*P<0.05$.

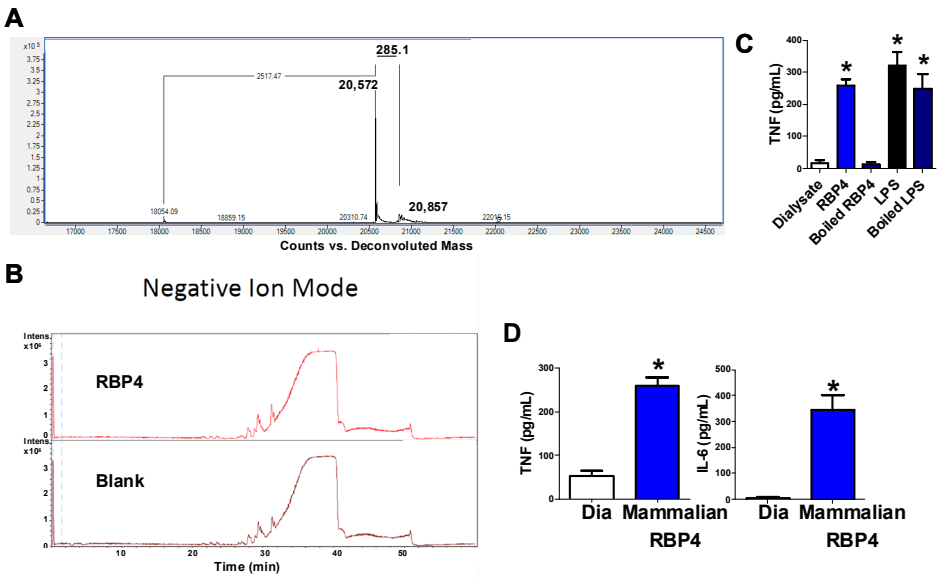

Figure S6, related to Figure 5. Experimental evidence for purity of recombinant RBP4. Mass spectrometry analysis of purified RBP4. (A) First, the sample was analyzed with and without strong cation exchange cleanup. This analysis detected a predominant peak corresponding to RBP4 not bound to retinol with a molecular weight of 20,572 Da. A very small peak was also detected which corresponded to RBP4-bound to retinol with a molecular weight of 20,857 Da. This excludes any protein contaminant. (B) Analysis of RBP4 in negative ion mode for high to low molecular weight lipids. This excludes any lipid or lipoprotein contaminant. (C) Recombinant RBP4 (50µg/mL) or LPS (100ng/mL) was boiled for 15 minutes. RBP4 and LPS (boiled or not boiled) was incubated with bone marrow derived dendritic cells for 24h and TNF secretion was measured by ELISA. This excludes LPS contamination. (D) RBP-4 produced in mammalian cells was incubated for 24h with bone marrow derived dendritic cells and TNF and IL-6 secretion were determined by ELISA. Values are means±standard error. Dia: dialysate control. *P<0.05 versus all other groups. This excludes bacterial-derived contaminants.

Table S1

Summary of the data confirming the purity of our RBP4 preparation, related to Figure 5.

Experimental approach:	Excludes:
1. Boiling RBP4 eliminates cytokine production (Figure S6C).	**LPS and other heat-sensitive protein or lipid contamination**
2. The endotoxin level of this recombinant RBP4 protein was less than 0.001 endotoxin unit per μg, which is the same as the ambient endotoxin levels in reverse-osmosis double-deionized water as previously described (Norseen et al., 2012).	**LPS contamination**
3. Polymyxin B (PMB) inhibits LPS-induced macrophage activation, but not RBP4-induced macrophage activation (data not shown).	**LPS contamination**
4. Organic extraction to generate RBP4 used in this study further removes other potential contaminants (Norseen et al., 2012).	**Bacterial derived contaminant**
5. RBP4 produced in mammalian cells induces cytokine secretion by dendritic cells (Figure S6D).	**Bacterial derived contaminant**
6. RBP4 purified from human blood induces cytokine secretion by dendritic cells (data not shown).	**Bacterial derived contaminant**
7. RBP4 overexpressing mice have increased cytokine production by ATMΦ.	**Any contaminant**
8. Mass spectrometry does not show any trace of protein, lipoprotein or lipid contamination (Figure S6A-B).	**Any contaminant**

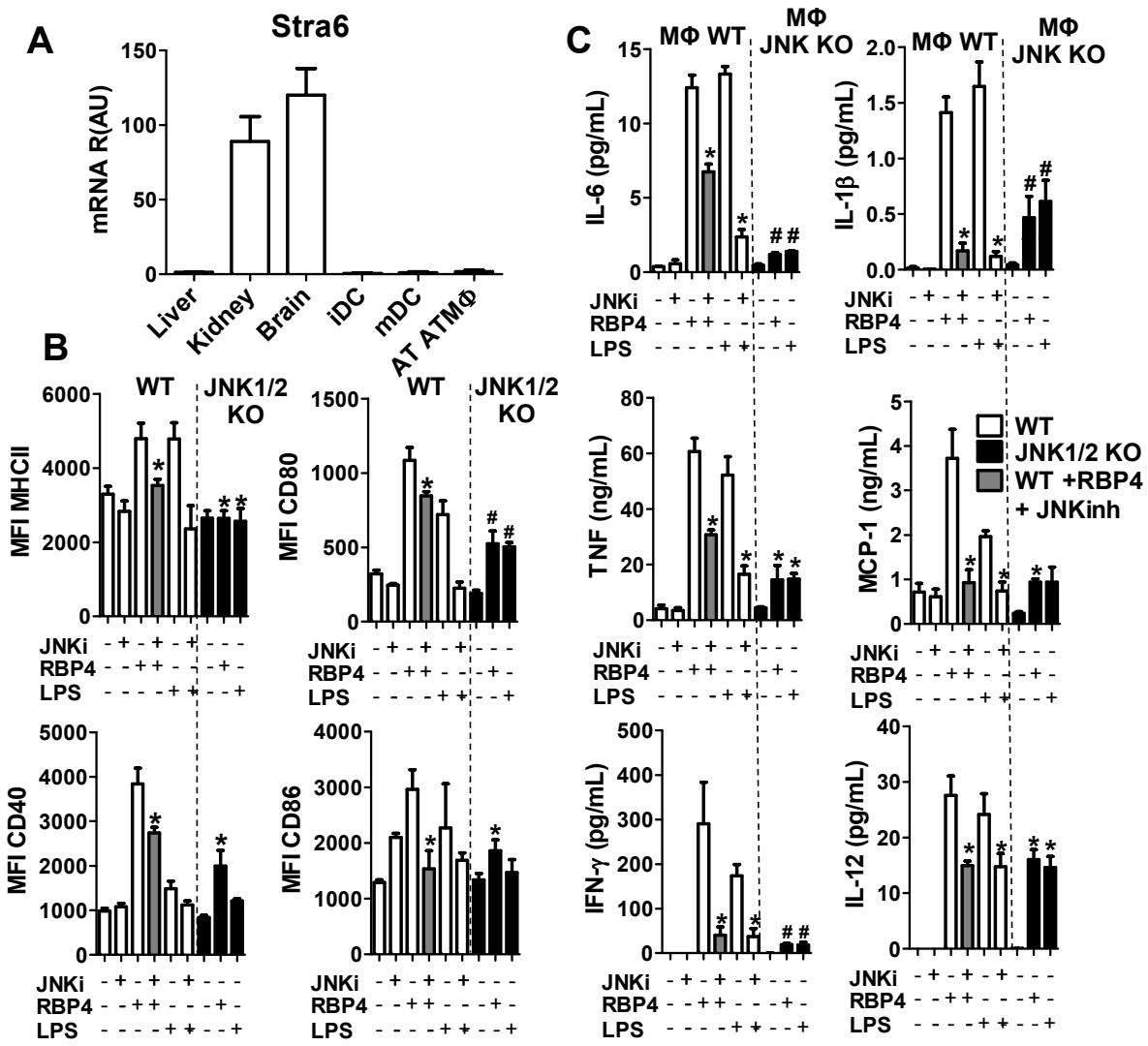

Figure S7, related to Figure 7. RBP4-induced activation of bone marrow derived macrophages is STRA6 independent and JNK1/2-dependent. (A) Stra6 mRNA levels were evaluated in bone marrow derived dendritic cell (both immature and mature) and in sorted adipose tissue macrophages by qPCR. Liver was used as a negative control and kidney and brain as positive controls (n=6/group). (B) Bone marrow derived macrophages from WT mice were treated with RBP4 (50 µg/mL for 24h). JNK inhibitor (JNKinh) (5µg/mL for 24h) or vehicle (DMSO) was added 30 minutes before RBP4 (50 µg/mL) stimulation where indicated. Bone marrow derived macrophages from mice with specific macrophage knockout of JNK1 and JNK2 (JNK1/2 KO) were treated with RBP4 (50 µg/mL for 24h). The levels of MHCII and co-stimulatory molecules (CD40,

CD80 and CD86) were measured by flow cytometry (n=4/group). (C) The levels of TNF, IL-6, IL-12 and IL-1β were measured in the supernatant of cultured macrophages as described in (B) (n=4/group). Values are means±standard error. *P<0.05 versus RBP4 or LPS treated group. $^{\#}P$<0.05 all other groups.

SUPPLEMENTAL EXPERIMENTAL PROCEDURES

Animal studies and measurement of metabolic parameters

Male RBP4-overexpressing (RBP4-Ox) mice on a C57BL6 background were bred with female C57BL6/J mice (Jackson Laboratories) to generate RBP4-Ox mice and control littermates. The RBP4-Ox mice express human-RBP4 under the control of mouse muscle creatine kinase (MCK) promoter and were extensively characterized (Quadro et al., 2002). 12-19 week old male mice were used for all studies. Macrophage-specific JNK1 and JNK2 knockout male mice (8 week old) were provided by Dr. Roger J. Davis and were previously described (Han et al., 2013). Mice were housed at Beth Israel Deaconess Medical Center with a 14/10 light-dark cycle and were fed standard chow diet (Formulab 5008). Blood collections were performed by tail vein bleeding. Body composition was measured by NMR (Echo Medical Systems). Insulin (ITT) and glucose (GTT) tolerance tests were performed in awake mice after a 5-h fast and a 12-h fast, respectively. GTT was accomplished by intraperitoneal (i.p.) injection of glucose (1 g glucose/kg body weight). ITT was performed in by i.p. injection of human regular insulin (0.8 U insulin/kg body weight; Lilly, Indianapolis, Indiana). Food was removed at 8 AM. Blood glucose was determined with a One Touch Basic glucometer (Lifescan, Milipitas, California). Mice were sacrificed by CO_2 euthanasia or decapitation and serum was collected. Next, mice were perfused with PBS and tissues harvested, snap frozen in liquid nitrogen, and stored at −80C for future processing or directly used for flow cytometry and subsequent *in vitro* studies. Mouse studies were conducted in accordance with federal guidelines. The Institutional Animal Care and Use Committee (Beth Israel Deaconess Medical Center, Boston, MA) approved all studies. All studies were performed on age- and sex-matched littermates.

Recombinant RBP4 preparation and treatment

Human RBP4 was expressed in *Escherichia coli* and purified as described previously (Yang et al., 2005). The endotoxin level of this recombinant protein was less than 0.001 endotoxin unit per µg, which is the same as the ambient endotoxin levels in reverse-osmosis double-deionized water as quantitatively measured by the *Limulus*amoebocyte lysate test (Lonza *Limulus* amoebocyte lysate QCL-1000; catalog no. 50-647 U). Moreover, boiled RBP4 lost the capacity to activate BMDC, indicating lack of endotoxin contamination. Moreover, purchased RBP4 (R&D system) produced in mammalian cell incubated with bone marrow DC induced cytokine secretion. To generate retinol-free RBP4, RBP4 was first incubated with 40% butanol–60% diisopropyl ether at 30°C overnight to remove retinol and centrifuged at 5,000 rpm for 5 min, and the bottom phase containing recombinant RBP4 was collected. This step was repeated twice more with 1-h incubations of 40% butanol–60% diisopropyl ether. RBP4 was purified by high-performance liquid chromatography (HPLC), and the protein quality measured both by Western blotting after separation by nondenaturing gel electrophoresis and by fluorescent spectrometry. After HPLC purification, RBP4 was dialyzed against 1× phosphate-buffered saline (PBS) for 4 h using a Slide A Lyzer dialysis cassette (Thermo Scientific). The retinol-free RBP4 remained retinol-free culture medium supplemented with fetal calf serum as previously described (Norseen et al., 2012). The dialysate buffer was used as a vehicle control in experiments where indicated. The protein was stored at −80°C and protected from exposure to light. RBP4 purity was verified by mass spectrometry with and without a strong cation exchange cleanup by the Small Molecule Mass Spectrometry Facility at Harvard University. Detergent removal was used to remove the neutral detergent under acidic conditions that bind the proteins to the SCX resin. The sample was then eluted at basic pH and analyzed by Liquid chromatography–mass spectrometry. Analysis of RBP4 was also done in negative ion mode under several tuning conditions optimized for high to low molecular weight.

Generation and RBP4 treatment of bone marrow-derived dendritic cells (BMDC)

Mouse bone marrow cells were flushed from the femurs and tibiae of 8-12 weeks old C57BL6/J male mice on a chow diet. The red blood cells were lysed with RBC lysis buffer (Biolegend), and the cells were plated in 6 wells flat bottom plate at a density of $1.0x10^6$ cells/mL in RPMI1640 (Gibco) containing 10% FBS (Gibco) and supplemented with essential amino acids, pyruvate, glutamine, vitamins, β-mercaptoethanol and antibiotics (Gibco). GM-CSF (R&D) at a concentration of 20 ng/mL was used for BMDC differentiation. The medium was replaced on day 4, and the cells were harvested on day 6 to obtain immature DC (non-activated – iDC). To obtain activated DC (mDC), RBP4 or LPS was added and the cells were cultured for an additional 24 h. LPS was used at a final concentration of 100 ng/mL. RBP4 was used at a final concentration of 1, 25 or 50 µg/mL. The dialysate buffer was used as a vehicle control in experiments where indicated.

Bead purification, cell sorting and co-culture assay

$CD4^+$ T cells from the spleen of donor C57B6/J male age matched mice and $CD11b^+$ cells from the perigonadal adipose tissue of RBP4-Ox or WT mice were purified by magnetic beads as described by the manufacture (Myotecny). AT stromal vascular fractions were stained with fluorescence-labeled antibodies for CD11b, Ly6C, F4/80, CD11c CD206 (Biolegend) and sorted at high speed (BD FACSAria II - Beth Israel Deaconess Medical Center Flow Cytometry Core). After sorting, cells purities were higher than 98%. Sorted M1 ATMΦ ($CD11b^+F4/80^+Ly6C^-CD11c^+CD206^-$) or M2 ATMΦ ($CD11b^+F4/80^+Ly6C^-CD11c^-CD206^+$) were plated at a density of 0.5 x 10^5 cells/U-bottom 96 well plate and co-cultured for 5 days with 2.0 x 10^5 splenic bead-purified cell trace violet - labeled CD4 T cells. The ratio of 1 APC to 4 CD4 T cell was chosen after co-culture titration. Anti-CD3 antibody (1ug/mL) (Biolegend) was used for polyclonal

stimulation of co-cultured CD4 T cells as previously described (Moraes-Vieira et al., 2013; Quintana et al., 2010). CD4 T cell proliferation was evaluated by cell trace violet (Invitrogen) dilution. Intracellular cytokine production (readout for CD4 T cell polarization) was determined after 5 days of culture and was assessed by flow cytometry as described (Moraes-Vieira et al., 2013; Quintana et al., 2010).

Flow cytometry of surface markers, intracellular cytokine and Foxp3 transcription factor

The AT stromal vascular fraction or BMDC cells were re-suspended in PBS supplemented with 2% FCS and surface markers were stained with saturating amounts of fluorescent labeled monoclonal antibody in combinations of 8-10 markers for multicolor flow cytometry (Table S2). For intracellular cytokine staining, cells were stimulated *in vitro* for 5 h at 37 °C in 5% CO_2 with leukocyte activation cocktail (BD Biosciences). The cells were permeabilized using the BD Cytofix/Cytoperm Fixation/Permeabilization kit (BD Biosciences). Intracellular staining was performed with saturating amounts of fluorescent labeled monoclonal antibody. To determine the frequency of Tregs ($CD4^+CD25^+Foxp3^+$) *in vivo*, AT stromal vascular fraction cells were stained intracellular for Foxp3 using an PE anti-mouse/rat Foxp3 antibody kit (eBioscience). The cells were acquired on specially ordered 5 lasers LSR II flow cytometer (BD Biosciences) at the Beth Israel Deaconess Medical Center Flow cytometry Core and analyzed with FlowJo 9.2.3 software (Treestar).

Table S2

Flow cytometry antibodies used in this study

Antibody	Clone	Company
CD209	PC61.5	eBioscience
IL-1β	NJTEN3	eBioscience
CD25	PC61.5	eBioscience
Foxp3	FJK-16s	eBioscience
CD44	IM7	Biolegend
CD69	H1.3F3	Biolegend
TNF	MP6-XT22	Biolegend
CD4	GK1.5	Biolegend
CD11c	N418	Biolegend
IL-6	MP5-20F3	Biolegend
IL-10	JES5-16E3	Biolegend
CD80	16-10A1	Biolegend
CD86	GL-1	Biolegend
CD11b	M1/70	Biolegend
CD40	23-Mar	Biolegend
I-A/I-E	M5/114.15.2	Biolegend
Ly6C	HK1.4	Biolegend
CD11c	N418	Biolegend
I-Ab (Iβb)	25-9-17	Biolegend
IL-12p40	C15.6	Biolegend
F4/80	CI:A3-1	Biolegend
CD62L	MEL-14	Biolegend
CD3	17A2	Biolegend
CD206	C068C2	Biolegend
Ly6G	1A8	Biolegend
IL-4	11B11	Biolegend
IFN-γ	XMG1.2	Biolegend
IL-17A	TC11-18H10.1	Biolegend
CD45	30-F11	BD Horizon
CD11b	M1/70	BD Horizon

$CD4^+$ T cell proliferation assay

FACS-Sorted M1 ($Ly6C^-CD11b^+F4/80^+CD11c^+CD206^-$) or M2 ($Ly6C^-CD11b^+F4/80^+CD11c^+CD206^-$) or bead-purified AT $CD11b^+$ cells or BMDC from WT C57B6/J (not activated - dialysate or activated with RBP4 or LPS) were co-cultured with cell trace violet-labeled bead-purified splenic syngeneic $CD4^+$ T cells from WT mice. Anti-CD3 antibody (Biolegend) was added. The cells were

cultured at 37 °C in 5% CO_2 for 5 days. Cell proliferation was quantified by flow cytometry. The expansion index was calculated with FlowJo 9.2.3 software.

Gene Expression analysis

RNA from M1 and M2 ATMΦ sorted from the AT pooled from 8-10 WT or RBP4-Ox mice was extracted using a RNeasy Mini Kit (Qiagen, USA) according to the manufacturer's instructions. The cDNA was synthesized using an RT2 First Strand Kit (Qiagen). Gene expression was analyzed in a 7900 HT thermocycler (TaqMan; Applied Biosystems). SDS 2.3 (Applied Biosystems) was used for calculation of cycle thresholds. Each sample was run in duplicate and relative expression levels determined using the $2^{-\Delta Ct}$ method with normalization of target gene expression levels to Gapdh (catalog number 4352339E, Applied Biosystems). Primers and probes were obtained from Applied Biosystems, and identification (ID) numbers for each gene are as follows: *Arg1* (Mm00475988_m1), *Cd11c* (Mm00498698_m1), *Il-1β* (Mm00434228_m1), Il6 (Mm00446190_m1), *Il-10* (Mm00439616_m1), *Nos*2 (Mm00440502_m1), *Mgl2* (Mm00460844_m1), *Mrc1* (Mm00485148_m1), *Pparγ* (Mm01184322_m1), *Il-12p40* (Mm00434174_m1) and *Tnf* (Mm00443258_m1). Mouse tissues were harvested following CO2 euthanasia or decapitation, snap frozen in liquid nitrogen, and stored at −80C for processing. Total RNA was extracted from frozen tissue with RNAeasy Lipid tissue mini kit (Qiagen). Reverse transcription was performed using RT2 First Strand Kit (Qiagen). Quantitative PCR was performed using SYBR Green PCR Master Mix (Applied Biosystems) in a 7900 HT thermocycler (Applied Biosystems). SDS 2.3 (Applied Biosystems) was used for calculation of cycle thresholds. Relative expression levels were determined using the $2^{-\Delta Ct}$ method with normalization of target gene expression levels to *Gapd*h. *Gata3*: 'CTGGGCCATTCGTACATGGAA' and GGATACCTCTGCACCGTAGC', *Rorc*: 'GACCCACACCTCACAAATTGA' and 'AGTAGGCCACATTACACTGCT'; *Gapdh*: 'AGGTCGGTGTGAACGGATTTG' and 'TGTAGACCATGTAGTTG AGGTCA'; *Foxp3*: 'CCCATCCCCAGGAGTCTT'

and ‘CCATGACTAGGG GCACT’; *Tbx21*: ‘AGCAAGGACGGCGAATGTT’ and ‘GGGTGGACAT ATAAGCGGTTC’.

APC transfer into WT recipient mice

BMDC cells were cultured for 6 d in the presence of GM-CSF (20 ng/mL). On day 6, the cells were treated with RBP4 (50µg/mL) or vehicle (dialysate), and 24 h later analyzed by flow cytometry to confirm BMDC activation. The cells were purified with $CD11c^+$ beads (Miltenyi). BMDC (non-activated – dialysate - iDC) and RBP4-activated BMDC (mDC) were injected i.p. into WT mice (3×10^6 per mouse) once a week for 6 weeks. PBS was injected as control. Three days after the last transfer of BMDC, fasting glucose levels were obtained and 5 days after the last transfer ITT was performed. The mice were sacrificed one week after the last cell transfer and the perigonadal AT stromal vascular fraction analyzed by flow cytometry.

Analytical procedures

Triglyceride levels were measured by colorimetric enzyme assays and free fatty acid levels were measured in serum using the NEFA-C kit (Wako, Richmond, Virginia). Cytokines (Il-12p70, IL-1β, IFN-γ, IL-6, and TNF-α) and MCP-1 secreted into conditioned medium were measured by ELISA according to the manufacturers' instructions (Biolegend). Serum insulin was measured by an ultra sensitive mouse insulin ELISA kit (Crystak Chem inc.) and adiponectin by a mouse adiponectin ELISA kit (Invitrogen) as manufacturers' instructions. RBP4 tissue and serum levels were measured by Western as previously described (Yang et al., 2005). Briefly, mouse proteins were detected using anti-mouse RBP4 polyclonal antibody (TAKEDA) and human RBP4 proteins were detected using anti-human RBP4 polyclonal antibody (DAKO). The anti-human antibody also recognizes mouse RBP4 but with lower affinity. Transgenic human RBP4 levels in the serum of RBP4-Ox mice were measured by a human RBP4 ELISA

Kit that does not detect mouse RBP4, following manufactur' instructions (AdipoGen).

Statistics

All values are given as means ± S.E.M. Differences among groups were compared using ANOVA with Tukey post-test for multiple comparisons and Student's t-test when there were only two groups. All statistical analyses were performed using GraphPad PRISM® 5 software, and the differences were considered significant when $P<0.05$.

SUPPLEMENTAL REFERENCES

Han, M.S., Jung, D.Y., Morel, C., Lakhani, S.A., Kim, J.K., Flavell, R.A., and Davis, R.J. (2013). JNK expression by macrophages promotes obesity-induced insulin resistance and inflammation. Science *339*, 218-222.

Moraes-Vieira, P.M., Bassi, E.J., Larocca, R.A., Castoldi, A., Burghos, M., Lepique, A.P., Quintana, F.J., Araujo, R.C., Basso, A.S., Strom, T.B.*, et al.* (2013). Leptin modulates allograft survival by favoring a th2 and a regulatory immune profile. Am J Transplant *13*, 36-44.

Norseen, J., Hosooka, T., Hammarstedt, A., Yore, M.M., Kant, S., Aryal, P., Kiernan, U.A., Phillips, D.A., Maruyama, H., Kraus, B.J.*, et al.* (2012). Retinol-binding protein 4 inhibits insulin signaling in adipocytes by inducing proinflammatory cytokines in macrophages through a c-Jun N-terminal kinase- and toll-like receptor 4-dependent and retinol-independent mechanism. Mol Cell Biol *32*, 2010-2019.

Quadro, L., Blaner, W.S., Hamberger, L., Van Gelder, R.N., Vogel, S., Piantedosi, R., Gouras, P., Colantuoni, V., and Gottesman, M.E. (2002). Muscle expression of human retinol-binding protein (RBP). Suppression of the visual defect of RBP knockout mice. J Biol Chem *277*, 30191-30197.

Quintana, F.J., Murugaiyan, G., Farez, M.F., Mitsdoerffer, M., Tukpah, A.M., Burns, E.J., and Weiner, H.L. (2010). An endogenous aryl hydrocarbon receptor ligand acts on dendritic cells and T cells to suppress experimental autoimmune encephalomyelitis. Proc Natl Acad Sci U S A *107*, 20768-20773.

Yang, Q., Graham, T.E., Mody, N., Preitner, F., Peroni, O.D., Zabolotny, J.M., Kotani, K., Quadro, L., and Kahn, B.B. (2005). Serum retinol binding protein 4 contributes to insulin resistance in obesity and type 2 diabetes. Nature *436*, 356-362.